Biosensors and Bioelectronics 304 (2026) 118571

Contents lists available at ScienceDirect

Biosensors and Bioelectronics

journal homepage: www.elsevier.com/locate/bios

On-site detection of airborne foodborne pathogens using a field-deployable recombinase polymerase amplification and CRISPR/Cas12a cleavage activity assay

Yeonwoo Jeong [a], Jina Lee [a,b], Sangsoo Choi [c], Dongmin Shin [c], Soojin Jang [a,b], Seong Uk Son [a,b], Taejoon Kang [a,d], Juyeon Jung [a,b,e], Jungho Hwang [c,*], Eun-Kyung Lim [a,b,e,f,**]

[a] Bionanotechnology Research Center, Korea Research Institute of Bioscience and Biotechnology (KRIBB), Daejeon, 34141, Republic of Korea
[b] Department of Nanobiotechnology, KRIBB School of Biotechnology, UST, Daejeon, 34113, Republic of Korea
[c] Department of Mechanical Engineering, Yonsei University, Seoul, 03722, Republic of Korea
[d] Graduate School of Medical Science and Engineering, KAIST, Daejeon, 34051, Republic of Korea
[e] School of Pharmacy, Sungkyunkwan University, Suwon, 16419, Republic of Korea
[f] YUHS-KRIBB Medical Convergence Research Institute, Yonsei University, Seoul, 03772, Republic of Korea

ARTICLE INFO

Keywords:
Food hygiene
Airborne bacteria detection
RPA–CRISPR/Cas 12a-based detection
Air sampling
Foodborne bacteria
Field-deployable detection

ABSTRACT

With the global increase in single-person households, the demand for meal kits is increasing, leading to the development of large-scale food production systems and complex supply chains. However, under the influence of global warming, these systems can be susceptible to food contamination, particularly by airborne foodborne bacteria. Conventional methods for detecting airborne bacteria involve complex, time-consuming, and labor-intensive processes, which limit their applicability for field use and rapid food hygiene surveillance. In the present study, we developed a field-deployable diagnostic platform by combining recombinase polymerase amplification with **C**RISPR/**C**as12a clea**V**age **A**ctivity (RCCVA assay) for the rapid and sensitive identification of airborne foodborne bacteria. Airborne bacteria were collected using a self-developed electrostatic air sampler and analyzed using a portable isothermal amplification device. The RCCVA assay was designed to detect four major foodborne pathogens: *Staphylococcus aureus*, *Salmonella enteritidis*, *Listeria monocytogenes*, and *Bacillus cereus*. The limit of detection was measured as 274.9, 4.5, 9.5, and 28.5 culture-forming units (CFU)/mL, respectively, within 45 min. This platform enables early on-site detection of airborne pathogens within approximately 1 h (for the analytical phase) and shows potential for real-time monitoring in food processing environments, thereby contributing to improved public health and food safety.

1. Introduction

With the global rise in single-person households, the demand for meal kits is also growing (Euromonitor International, 2020; U.S. Census Bureau, 2023; Eurostat, 2025). This trend has driven the development of large-scale food production systems and the expansion of complex supply chains (Badia-Melis et al., 2018; James, 2023). However, under the influence of global warming, these systems are becoming more vulnerable to food contamination and spoilage. Food poisoning, the most well-known outcome of such contamination, poses a significant threat to public health, causing approximately 420,000 deaths annually (World Health Organization, 2024). Therefore, food contamination must be systematically managed throughout the entire production and distribution process, and early, field-based detection of food poisoning bacteria in food facilities is essential. According to the *Bad Bug Book* published by the U.S. Food and Drug Administration (FDA), various bacterial strains are responsible for food poisoning, and among these, several can be transmitted through the air and are categorized as

* Corresponding author.
** Corresponding author. Bionanotechnology Research Center, Korea Research Institute of Bioscience and Biotechnology (KRIBB), Daejeon, 34141, Republic of Korea.
E-mail addresses: hwangjh@yonsei.ac.kr (J. Hwang), eklim1112@kribb.re.kr (E.-K. Lim).

https://doi.org/10.1016/j.bios.2026.118571
Received 16 December 2025; Received in revised form 6 February 2026; Accepted 27 February 2026
Available online 28 February 2026

airborne bacteria. For instance, *Staphylococcus aureus* has been detected in the air of contaminated environments such as hospitals, wastewater treatment facilities, and livestock farms (Kozajda et al., 2019). *Salmonella enteritidis* is known to contribute to airborne contamination, particularly through poultry and other birds (Gast et al., 1998, 2004). In addition, airborne *Listeria monocytogenes* poses a significant threat to the red meat processing industry (Dobeic et al., 2011), whereas *Bacillus cereus* is recognized as a volatile and pathogenic bacterium (Bottone, 2010). In addition, airborne transmission and infection cases of food poisoning bacteria have been reported in several studies, revealing a potential route of contamination within the food chain (Oliveira et al., 2006; Stein and Chirilă, 2017; Yong et al., 2024). Therefore, effective control of airborne bacteria is crucial for protecting public health. To date, various on-site airborne bacterial detection methods have been developed to ensure air safety (Qiu et al., 2023; Yong et al., 2024). However, in most cases, collected air samples require an additional culture step prior to identification and analysis. To overcome the complexity and time consumption associated with bacterial culture, proteomic-and nucleic acid-based analytical techniques have been introduced (Anaya et al., 2007; Chen et al., 2023; Qiu et al., 2023; Quijano-Rubio et al., 2021). Among these, polymerase chain reaction (PCR) and real-time PCR are the most-widely used and are recognized as gold-standard nucleic acid-based molecular diagnosis techniques (Chen et al., 2023; Pogner et al., 2024; Unterwurzacher et al., 2018; Watt et al., 2020). However, these techniques have inherent limitations, including the need for skilled personnel, labor-intensive procedures, extended processing time, and dependence on complex thermal cycling instruments equipped with fluorescence detection systems. As an alternative, isothermal amplification methods including loop-mediated isothermal amplification (LAMP), rolling circle amplification (RCA), recombinase polymerase amplification (RPA), exponential amplification reaction (EXPAR), and nucleic acid sequence-based amplification (NASBA) are widely used (Food and Drug Administration, 2020; Glökler et al., 2021; Huang et al., 2018; Li et al., 2017; Liu et al., 2021; Seo et al., 2025; Song et al., 2019; Wang et al., 2024; Yang et al., 2019; Yao et al., 2024; Zhao et al., 2015; Zheng et al., 2025). For example, a LAMP-mediated SARS-CoV-2 detection method was approved by the U. S. FDA in 2020 (Food and Drug Administration, 2020). Moreover, LAMP has been used to detect various pathogens across different applications. For instance, Huang et al. detected virulence genes of *E. Coli* O157:H7 and *Salmonella enterica* in food samples using LAMP (Huang et al., 2018). RCA-based methods have been reported for the detection of *Cronobacter sakazakii, Vibrio parahaemolyticus,* and *S. aureus* (Liu et al., 2021; Song et al., 2019; Yang et al., 2019). RCA amplicons can facilitate DNAzyme formation, such as G-quadruplex structures, which can generate detectable signals (Seo et al., 2024; Song et al., 2019). Another method, RPA, has also been widely adopted for the detection of foodborne bacteria owing to its simplicity and rapid amplification under isothermal conditions (Fu et al., 2025; Liu et al., 2022; Wang et al., 2020; Zhang et al., 2025). Molecular diagnostic systems based on clustered regularly interspaced short palindromic repeats (CRISPR) and their associated protein complexes (CRISPR/Cas) have gained significant attention because of their programmability and high target specificity (Ki et al., 2023; Li et al., 2023; Song et al., 2023; Yang et al., 2023). To enhance signal transduction, the CRISPR/Cas system is generally used in combination with other target amplification methods. Building on this strategy, Yan et al. integrated RCA with the CRISPR/Cas12a system to develop a one-pot assay for the sensitive detection of miRNA from extracellular vesicles (Yan et al., 2023). Similarly, Chen et al. combined RCA with CRISPR/Cas12a to detect *Escherichia coli* O157:H7 through electrochemical signal (Chen et al., 2021). Liu et al. also reported the use of RPA with CRISPR/Cas12a for detecting *Salmonella* spp. in food matrices (Liu et al., 2022). Zhang et al. developed a dual-mode sensing platform for *Mycobacterium tuberculosis* by combining RPA with the CRISPR/Cas system (Zhang et al., 2025). The fluorescence probe was quenched by gold nanoparticles (AuNPs), and upon target recognition, the CRISPR/Cas system released the fluorescence probe from the AuNPs, restoring fluorescence. Similarly, Arshad et al. used the RPA/CRISPR-Cas12a system with a CeO_2 nanozyme as a signal reporter to detect *Salmonella* spp. (Arshad et al., 2024). Although significant advancements have been made, the application of the RPA-CRISPR/Cas system for on-site detection of airborne bacteria remains underexplored. Therefore, we used the RPA-CRISPR/Cas system for the detection of airborne food poisoning bacteria. Airborne bacteria were collected using an electrostatic air sampler and subsequently analyzed with a portable isothermal amplification device. RPA/CRISPR-based reagents were designed and developed to specifically detect four major foodborne pathogens: *S. aureus*, *S. enteritidis*, *L. monocytogenes*, and *B. cereus*. After collecting airborne bacteria, the developed Recombinase polymerase amplification (**R**PA)-**C**RISPR/**C**as12a clea**V**age **A**ctivity assay (RCCVA assay) was used for rapid on-site analysis (Fig. 1).

2. Result & discussion

2.1. Performance evaluation of the RPA primer and crRNA in the RCCVA assay

For the RCCVA assay, the RPA primers were first designed to target bacterial virulence genes associated with foodborne pathogens, including *LukE* for *S. aureus*, *invA* and *pipD* for *S. enteritidis*, *EntFM* for *B. cereus,* and *actA* and *plcB* for *L. monocytogenes*. The RPA primers and crRNAs with their binding sites are illustrated in Figs. 2a, 3a, 4a,5a. The corresponding RPA primer sequences are listed in Table S1. To verify the specific reactivity of each RPA primer set, 10 ng of gDNA extracted from each bacterial strain was used as the template for the RPA reaction. As shown in the agarose gel images in Figs. 2b,3b,4b,5b, the *LukE* primer set for *S. aureus*; the invA1, invA2 and pipD primer sets; the invA2F and invA2-2 R combination for *S. enteritidis*; and all primer sets for *L. monocytogenes* and *B. cereus* generated amplicons of the expected sizes in the presence of their respective target DNA. Furthermore, the target amplicons confirmed by successful RPA amplification were analyzed using the CRISPR/Cas12a system, which specifically recognizes the RPA products generated by the validated primers and activates collateral cleavage of a fluorescent reporter, thereby generating a detectable fluorescence signal through a fluorescence resonance energy transfer (FRET) effect (Ha et al., 1996; Ki et al., 2023; Zhao et al., 2024). Once the Cas12a–crRNA complex is formed, recognition of the target amplicon containing the 5′-TTTV PAM sequence activates its collateral cleavage activity, leading to nonspecific cleavage of single-stranded DNA (ssDNA). The reporter ssDNA consisted of a fluorophore (fluorescein amidite, FAM) and a quencher (black hole quencher, BHQ) connected by a short ssDNA linker, which suppressed fluorescence through the FRET effect (Table S2). Upon activation, the Cas12a–crRNA complex cleaves this linker, resulting in recovery of the FAM fluorescence signal. The crRNA was designed to target the RPA amplicon with the assistance of the CRISPRscan program (http://CRISPRscan.org) (Fig. 6), and the corresponding sequences are listed in Table S2. Next, the selectivity of the designed crRNAs was verified using the CRISPR/Cas12a assay with a real-time PCR system. RPA amplicons generated from primer sets producing bands, with or without target gDNA, as well as deionized water as a control, were tested. As shown in Figs. 2c,3c,4c,5c, fluorescence signals (RFU) were observed only in the presence of RPA amplicons generated with target gDNA, whereas no signal was detected in no-target RPA amplicons or buffer-only controls. These results reveal that the crRNA binds to the target amplicon with high specificity, thereby activating the Cas12a–crRNA complex, which in turn cleaves the reporter ssDNA and generates a fluorescence signal. Among these results, the experimental groups with rapid initial signal amplification kinetics and small deviations were selected to evaluate the sensitivity of the RCCVA assay. Ten-fold serial dilutions of bacterial gDNA ranging from 1 ng/μL to 1 ag/μL were tested using a real-time PCR system (Figs. 2d,3d,4d,5d). Finally, the most sensitive combinations were

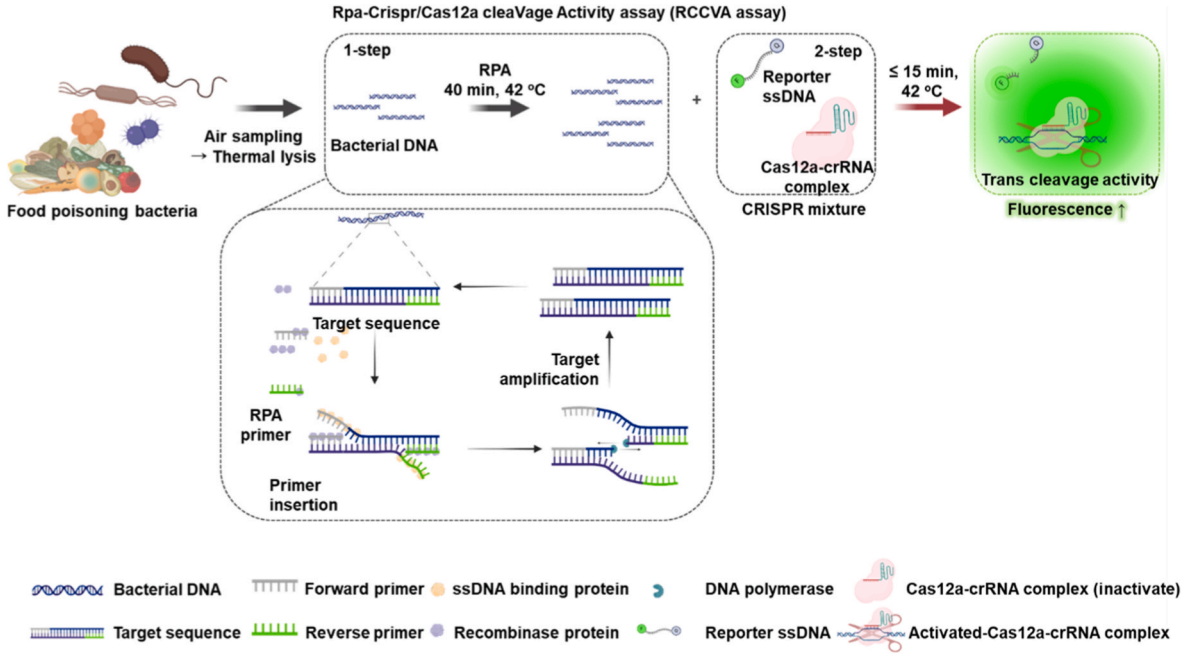

Fig. 1. Schematic illustration of the Recombinase Polymerase Amplification-CRISPR/Cas12a Activity (RCCVA) assay for rapid on-site detection of food-borne pathogens.

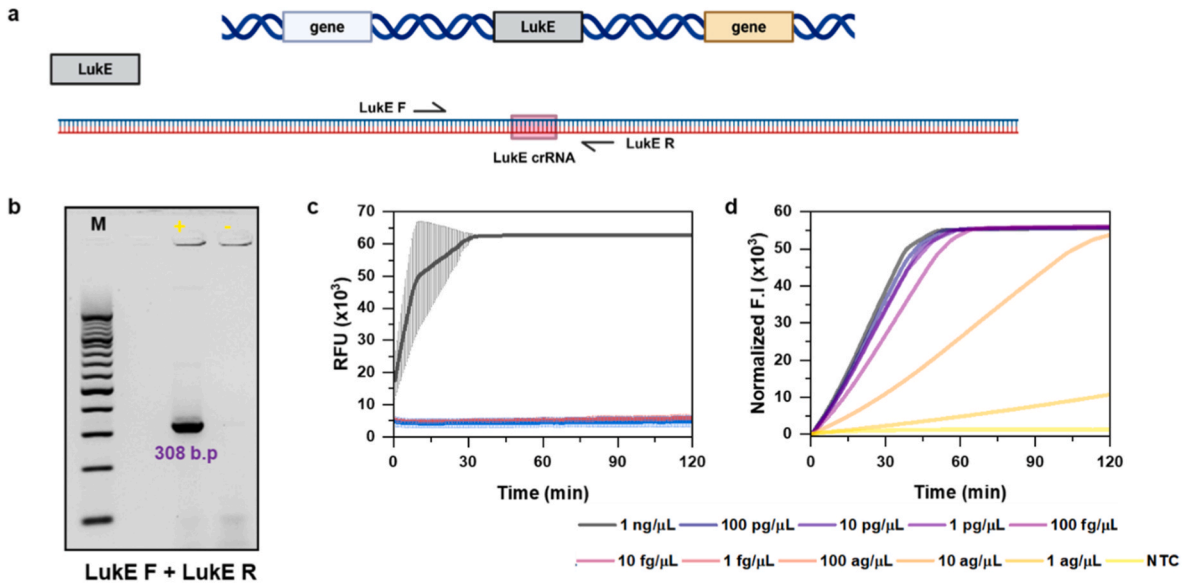

Fig. 2. Evaluation of the RCCVA assay for *Staphylococcus aureus* (*S. aureus*) detection. (a) Schematic representation of Recombinase Polymerase Amplification (RPA) primer locations and CRISPR RNA (crRNA) binding sites targeting *S. aureus*. **(b)** Agarose gel electrophoresis of RPA amplicons generated using the LukE primer set. Lanes: 100 bp DNA ladder (far left), (+) target gDNA, and (−) no-template control (NTC). **(c)** Kinetic analysis of CRISPR/Cas12a signal amplification using real-time PCR. Each reaction was measured in triplicate, with mean values shown as bold lines and error bars representing standard deviations (SD; black: RPA with target; red: RPA without target; blue: deionized water). (d) Kinetic analysis of CRISPR/Cas12a activation using selected crRNA and serial dilutions of *S. aureus* RPA amplicons. Each data point represents the mean of triplicate measurements.

selected as follows: the LukE primer set with LukE crRNA for *S. aureus*; invA2F and invA2-2R primer with invA2 crRNA for *S. enteritidis*, plcB3F and plcB2R with plcB2 crRNA for *L. monocytogenes*; and EntFM2F and EntFM2-2R with EntFM2 crRNA for *B. cereus* (Fig. S1). The corresponding RPA amplicon sizes were 308 bp, 236 bp, 167 bp, and 343 bp for *S. aureus, S. enteritidis, L. monocytogenes,* and *B. cereus*, respectively. In addition, the cross-reactivity of each RPA primer set was evaluated. RPA reactions were performed using genomic DNA from all tested bacterial strains with each primer set. No cross-reactivity was observed, indicating that the RPA primers and crRNAs used here exhibit high specificity without nonspecific amplification of non-target bacterial strains (Fig. S2). We also confirmed that the premixed assay reagents retained their performance for up to 1 month when stored at −20 °C (Fig. S3)

2.2. Validation of RCCVA assay using portable isothermal amplification device

Building on the discussions presented in the previous section, further experiments were conducted to evaluate the sensitivity of the RCCVA

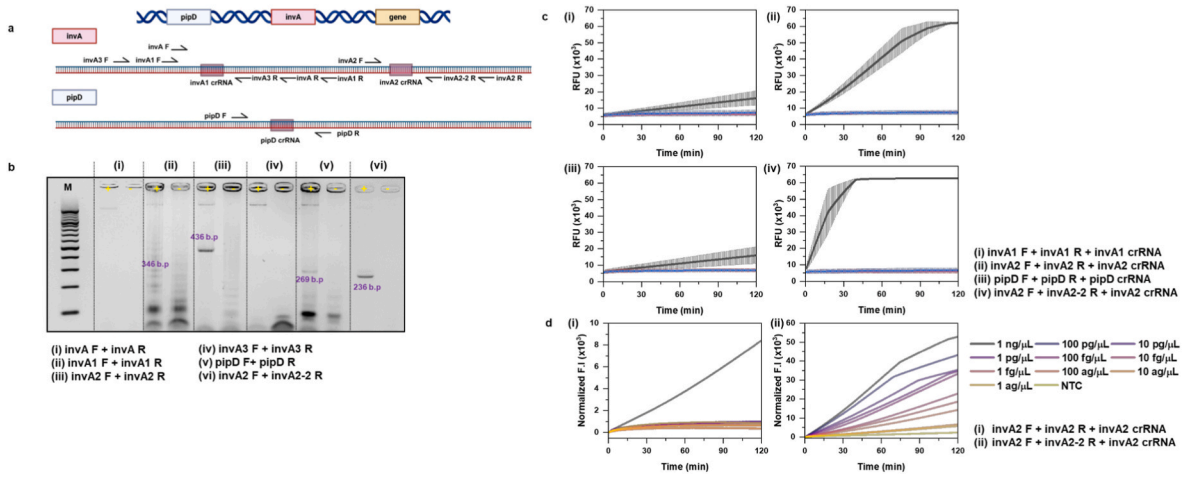

Fig. 3. Evaluation of the RCCVA assay for *Salmonella enteritidis* (*S. enteritidis*) detection. (a) Schematic illustration of RPA primer binding sites and crRNA targeting regions for *S. enteritidis*. **(b)** Agarose gel images of RPA amplicons generated using different primer sets. Lanes: 100 bp DNA ladder (far left), (+) target gDNA, and (−) NTC. **(c)** Kinetic analysis of CRISPR/Cas12a fluorescence amplification measured using real-time PCR. Triplicate measurements are shown, with mean signals depicted as bold lines and error bars representing standard deviations (SD; black: RPA with target; red: RPA without target; blue: deionized water). **(d)** Kinetic analysis of CRISPR/Cas12a activation using the selected crRNA and varying concentrations of RPA amplicon. Each value represents the mean of three replicates.

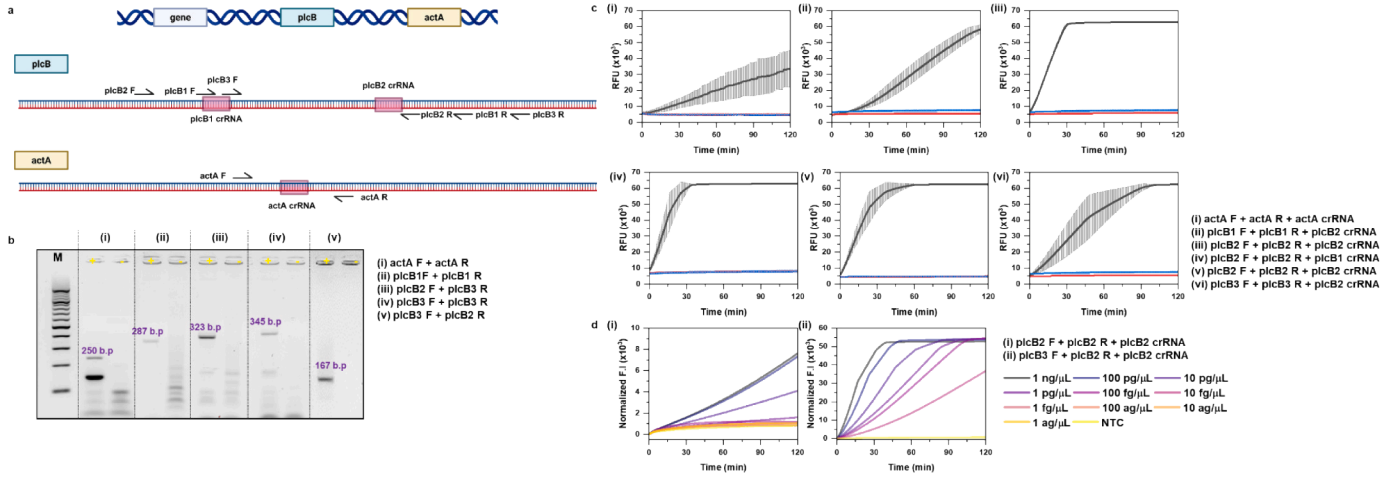

Fig. 4. Evaluation of the RCCVA assay for *Listeria monocytogenes* (*L. monocytogenes*) detection. (a) Schematic diagram of RPA primer positions and crRNA binding regions for *L. monocytogenes*. **(b)** Agarose gel electrophoresis of RPA products generated with each primer set. Lanes: 100 bp DNA ladder (far left), (+) target gDNA, and (−) NTC. **(c)** Fluorescence kinetics of CRISPR/Cas12a activation monitored using real-time PCR. Triplicate measurements are shown with mean signals as bold lines and error bars indicating standard deviations (SD; b lack: RPA with target; red: RPA without target; blue: deionized water). **(d)** Kinetic analysis of CRISPR/Cas12a fluorescence response using the selected crRNA and multiple concentrations of *L. monocytogenes* RPA amplicons, with each point representing the mean of three replicates.

assay. Serial 10-fold dilutions of bacterial gDNA ranging from 1 ng/μL to 1 ag/μL were tested using a portable isothermal amplification device, and the LOD was determined. The kinetics of the fluorescence signal corresponding to various gDNA concentrations were measured using the portable isothermal amplification device. A graph of normalized fluorescence intensity (F.I) over time was obtained (Fig. 7a), and the kinetics were analyzed at 15 min intervals (Fig. S4). As shown in Fig. 7a and Fig. S4, the normalized F.I increased with higher gDNA concentrations, and the amplification kinetics were clearly distinguishable across concentrations. The variation in detection sensitivity among bacterial species is primarily attributed to differences in the amplification efficiency of RPA primers and the characteristics of target genes. RPA is known to be highly sensitive to primer sequences. Although highly sensitive and specific primer sets were selected, factors such as the copy number of the target gene, genomic context, or sequence-specific accessibility can influence amplification efficiency (Daher et al., 2016). For instance, some genes may exist as multiple copies or be more accessible to primers, whereas others are present as a single copy or possess secondary structures that hinder primer binding (Daher et al., 2016; Piepenburg et al., 2006). Because RPA operates without a denaturation step, primers must invade double-stranded DNA, making amplification more susceptible to sequence composition and local DNA breathing dynamics. For example, AT-rich regions facilitate primer invasion, whereas GC-rich regions form more stable duplexes that reduce accessibility. Therefore, despite the target gene being present as a single copy and using the same bacterial concentrations as those used in the RCCVA assay, structural factors may limit primer accessibility, resulting in difference in detection sensitivity. Although partial deviations from linearity were observed in the relationship between F.I and gDNA concentration, the LOD for each bacterial strain was determined based on the range of data at the 15 min time point exhibiting the highest linear correlation (R^2). Consequently, the regression equations for the calibration curves were as follows: *S. aureus*: $y = 0.34x + 0.71$ ($R^2 = 0.9105$), *S. enteritidis*: $y = 0.05x + 0.30$ ($R^2 = 0.9433$), *L. monocytogenes*: $y = 0.39x + 0.34$ ($R^2 = 0.9280$), and

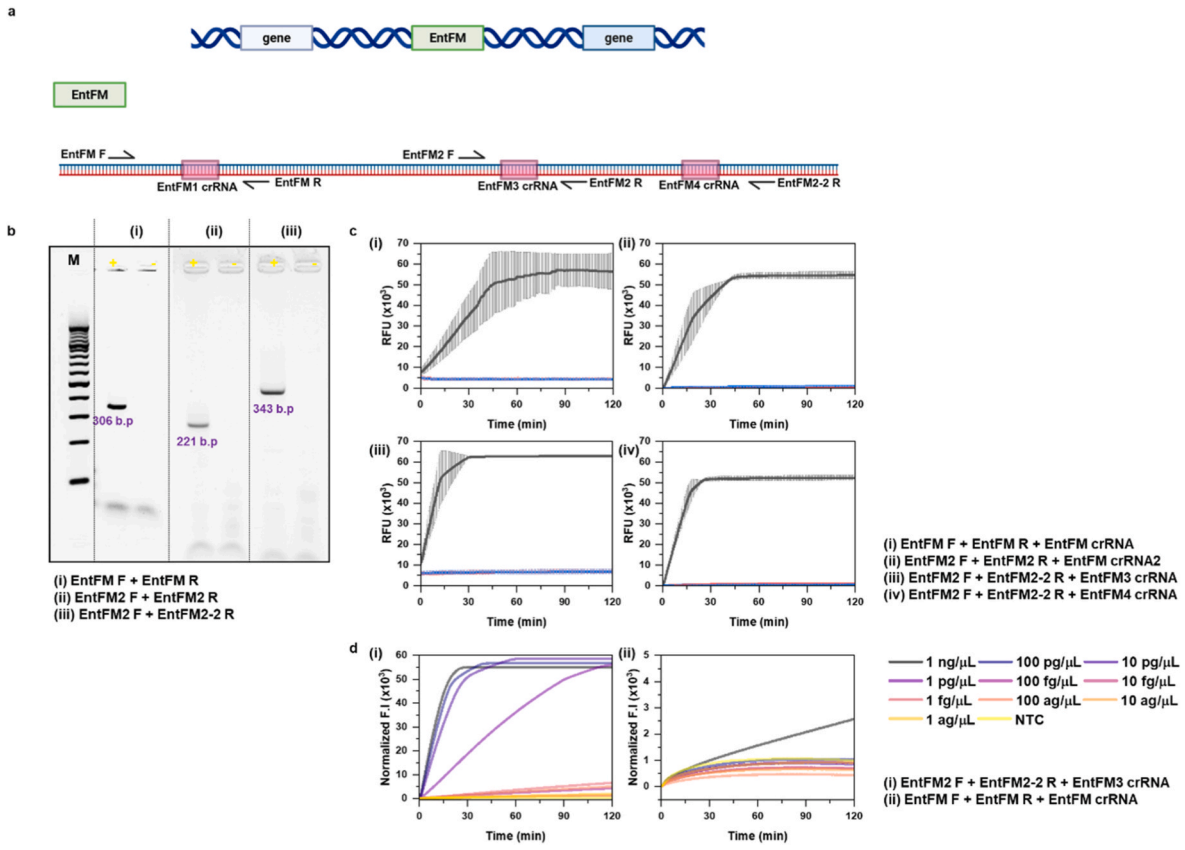

Fig. 5. Evaluation of the RCCVA assay for *Bacillus cereus* (*B. cereus*) detection. (a) Schematic illustration of RPA primer positions and crRNA binding sites targeting *B. cereus*. **(b)** Agarose gel electrophoresis of RPA amplicons generated using each primer set. Lanes: 100 bp DNA ladder (far left), (+) target gDNA, and (−) NTC. **(c)** Kinetic analysis of CRISPR/Cas12a fluorescence amplification using real-time PCR. Each reaction was performed in triplicate; mean values are shown as bold lines, with error bars representing standard deviations (SD; black: RPA with target; red: RPA without target; blue: deionized water). (**d)** Kinetic analysis of CRISPR/Cas12a activation using the selected crRNA and serial dilutions of *B. cereus* RPA amplicons. Each point represents the mean of triplicate measurements.

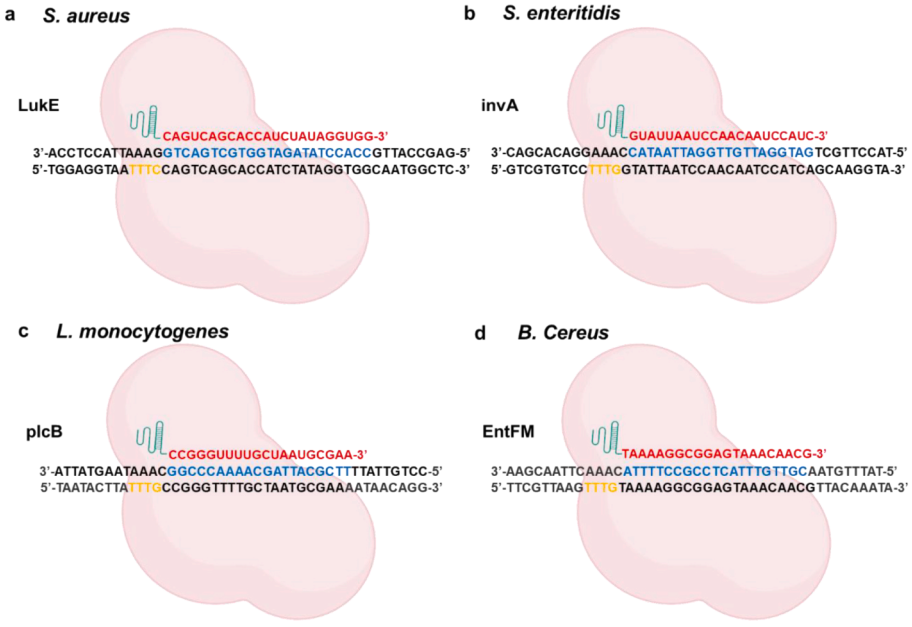

Fig. 6. Schematic illustration of the activated Cas12a–crRNA complex. Designed crRNA sequences, target sequences, and Protospacer Adjacent Motif (PAM) regions are indicated in red, blue, and orange, respectively.

B. cereus: y = 0.28x – 0.11 (R^2 = 0.9454), all of which showed strong linearity. Accordingly, the calculated LODs were 0.96 ag/μL, 1.64 fg/μL, 5.6 ag/μL, and 4.24 fg/μL for *S. aureus*, *S. enteritidis*, *L. monocytogenes*, and *B. cereus*, respectively, indicating that this RCCVA assay is capable

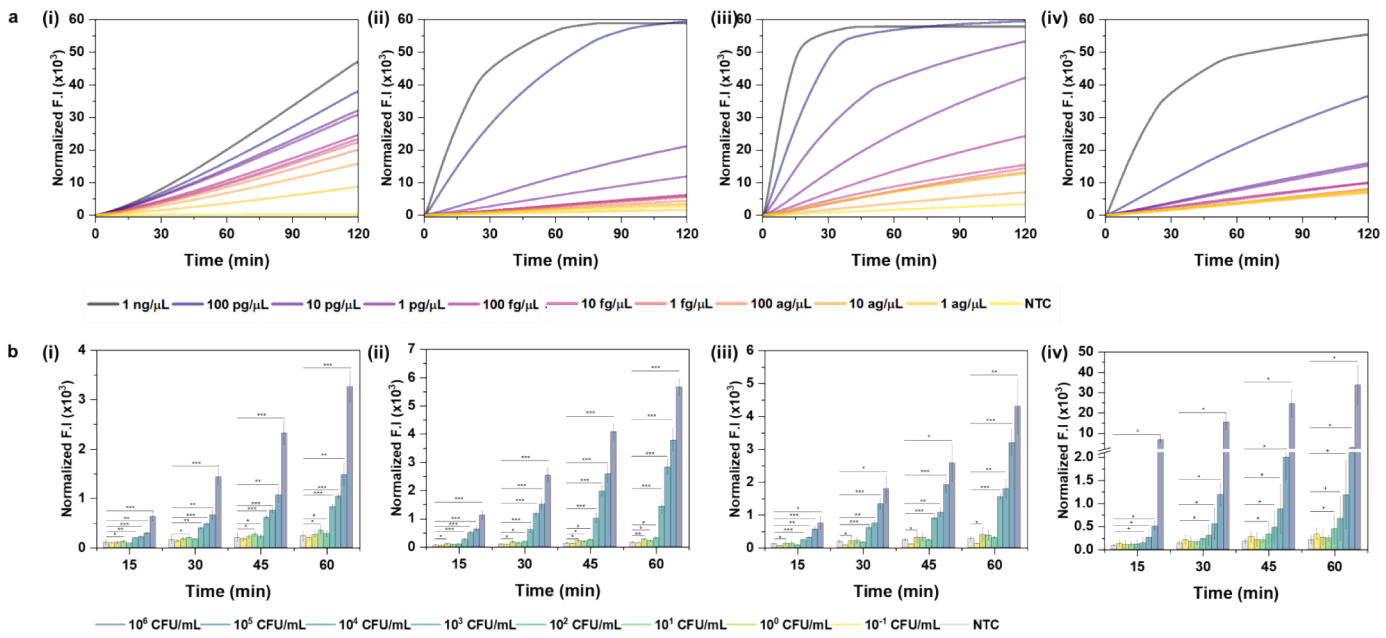

Fig. 7. Kinetics of the RCCVA assay using a portable isothermal amplification device. (a) Fluorescence kinetics obtained from varying concentrations of RPA amplicons for each bacterial strain. **(b)** Fluorescence kinetics from thermally lysed bacteria measured every 15 min: (i) *S. aureus*, (ii) *S. Enteritidis*, (iii) *L. monocytogenes*, and (iv) *B. cereus*. Each sample was analyzed in triplicate, and mean values are presented with standard deviations (SD). Significance levels: (−) $P < 0.2$, (+) $P < 0.1$, *$P < 0.05$, **$P < 0.01$, ***$P < 0.005$).

of quantitatively detecting extremely low concentrations of pathogenic genetic material.

2.3. Performance evaluation of RCCVA assay using thermally lysed bacteria

As an additional assessment for field deployment, the RCCVA assay was applied directly to heat-treated bacterial samples without DNA purification, allowing detection using gDNA released through thermal lysis. After heat-treating bacterial samples at various concentrations at 95 °C for 5 min, detection was performed using this assay. The increase in fluorescence intensity over the reaction time was measured at 15 min intervals, and each fluorescence value was normalized by subtracting the initial signal measured before the reaction started. As shown in Fig. S4, the strongest fluorescence signal was measured at the highest bacterial concentration (10^7–10^8 culture-forming units [CFU]/mL). Furthermore, even at low concentrations ranging from 10–10^1 CFU/mL, each target bacterium was clearly detectable based on fluorescence signals distinguishable from those of the NTC (Fig. 7b). Fluorescence intensities measured from bacterial concentrations at 10^{-1}–10^6 CFU/mL were used to evaluate the LOD for each assay. The calibration curves and corresponding linear regression equations based on the fluorescence values measured at the 1 h time point are as follows: 0.25x + 0.09 ($R^2 = 0.9062$), 1.38x - 2.72 ($R^2 = 0.9877$), 0.7x - 0.59 ($R^2 = 0.9058$), 1.02x – 2.47 ($R^2 = 0.8416$) for *S. aureus*, *S. enteritidis*, *L. monocytogenes*, and *B. cereus*, respectively. The corresponding LODs were 18.01, 1.14, 1.56 and 3.07 CFU/mL, respectively (Fig. S6). Even within a short measurement time of 15 min, the linear regression equations based on the fluorescence values measured were as follows: 0.05x + 0.05 ($R^2 = 0.8290$), 0.06 - 0.06 ($R^2 = 0.9777$, 0.12x - 0.12 ($R^2 = 0.8006$), 0.18x - 0.41 ($R^2 = 0.9596$) the LOD were determined to be 274.9, 4.5, 9.5, and 28.5 CFU/mL, respectively (Fig. S5b). The enrichment capacity of the air sampler to be used in subsequent experiments was reported as 2.7×10^5 (An et al., 2024). Accordingly, when the concentrations were converted to CFU/m^3, the corresponding values were calculated as 1.02×10^3, 16.8, 35.0, and 1.06×10^2 CFU/m^3 respectively. These findings revealed that this assay enables rapid and highly sensitive detection of target bacteria within a short time. Therefore, it was further applied to detect airborne food poisoning bacteria.

2.4. Airborne food poisoning bacteria detection using RCCVA assay

Airborne food poisoning bacteria were analyzed using the RCCVA assay. Aerosolized bacteria were collected using the Bioaerosol-to-Liquid Sampler (BALS-100, ART Plus, Ltd., Korea). To simulate airborne contamination conditions, four bacterial strains were aerosolized (Fig. 8), and the air was subsequently collected using the air sampler (Fig. 8a–c). The airborne bacteria entering the sampler were positively charged by ions generated from the discharge electrodes through corona discharge at an applied voltage of 10 kV (An et al., 2024). The charged bacteria were subsequently collected on a grounded electrode covered with 25 mL of phosphate-buffered saline (PBS) under the influence of the electric field. After sampling, the collected liquid was automatically transferred into a collection vial by an integrated peristaltic pump and then concentrated by centrifugation at 4000 rpm for 20 min. Each sample was subsequently subjected to thermal lysis at 95 °C for 5 min, followed by the RCCVA assay (Fig. 8d).

Although the same concentration of bacteria was added to each experimental group, the detection sensitivity varied among different bacterial species. These differences are because of species-specific variations in cell aggregation behavior during cultivation, aerosolization, and liquefaction, which can influence the release efficiency of genomic DNA during thermal lysis. For example, bacteria exhibiting strong intercellular adherence may be less susceptible to complete cell disruption and DNA release under heat treatment. Despite differences in DNA extraction efficiency, the thermal lysis method is advantageous for field-deployable applications, eliminating the need for complex DNA extraction steps (Thatcher, 2015; Shetty et al., 2017; Seo et al., 2024; Jeong et al., 2025). In addition, the variability may increase owing to the lack of a clearly defined reaction termination point when using the portable isothermal amplification device. Residual active enzymes that continue to react after amplification can influence the final F.I, resulting in greater signal variation. However, statistical analysis confirmed that the F.I. values of the positive samples were significantly higher than

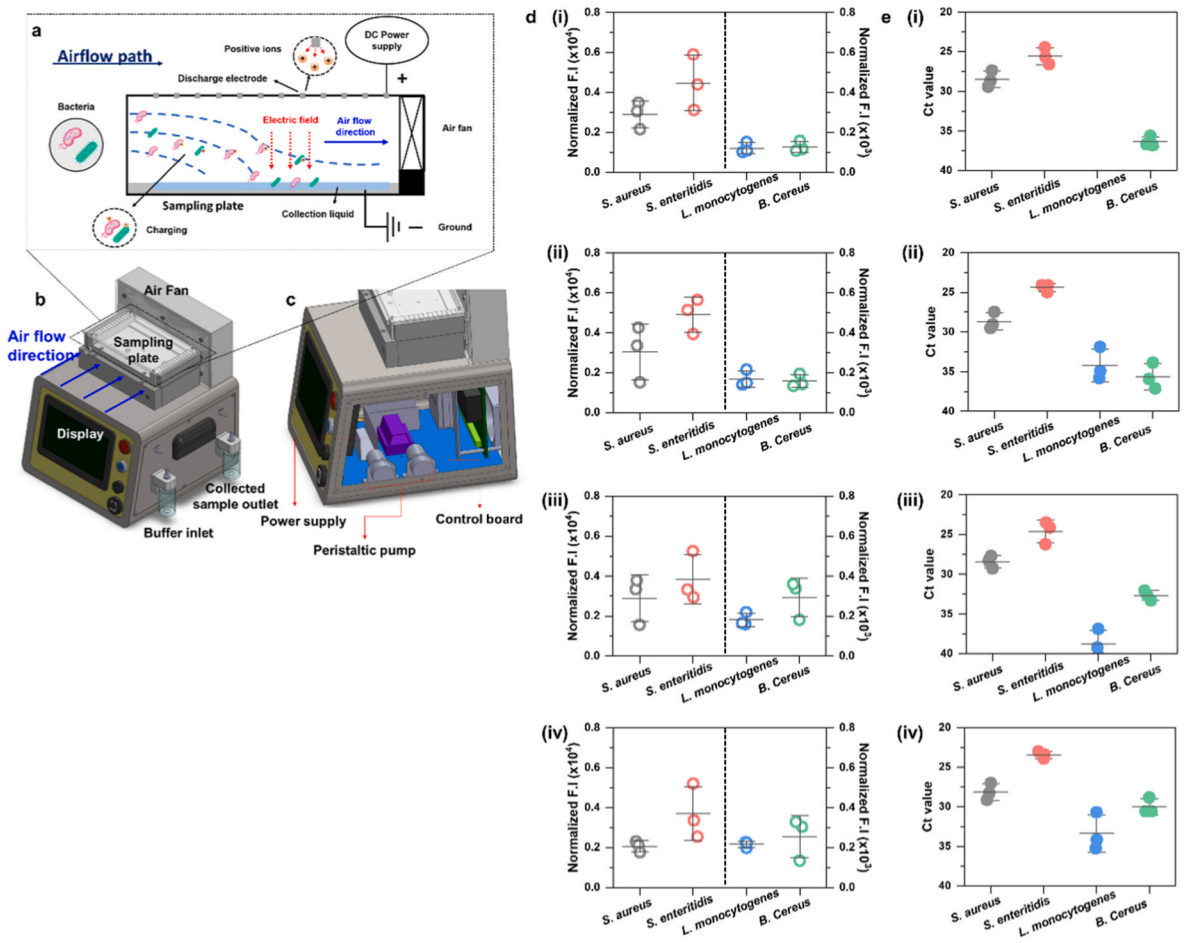

Fig. 8. Airborne bacterial detection using the air sampler and RCCVA assay compared with Real-time Polymerase Chain Reaction (RT-PCR). **(a)** Schematic workflow of airborne bacterial collection using the electrostatic air sampler. **(b)** Three-dimensional (3D) model of the sampling device (full view). **(c)** Internal left-side view of the device. **(d)** Normalized fluorescence intensity (F.I) at 15 min obtained from the RCCVA assay for air-collected samples. **(e)** Corresponding RT-PCR results. Samples contained aerosolized mixtures of: (i) *S. aureus* + *S. enteritidis*; (ii) *S. aureus* + *S. enteritidis* + *L. monocytogenes*; (iii) *S. aureus* + *S. enteritidis* + *B. cereus*; (iv) *S. aureus* + *S. enteritidis* + *L. monocytogenes* + *B. cereus*. Values represent triplicate measurements; error bars show standard deviations (SD).

those of the NTC, indicating reliable positive detection (Table S4). Despite the higher variability compared with real-time PCR, these results reveal that RCCVA can still reliably discriminate positive samples under field-applicable conditions, highlighting its potential for rapid on-site bacterial detection.

Furthermore, the same samples were analyzed using real-time PCR, the gold-standard method, to evaluate the reliability and performance of this assay (Fig. 8e). Overall, the fluorescence signals were consistent with the bacterial composition of each sample mixture, showing the reliable detection performance of this assay. The detection patterns showed a strong correlation with those obtained from real-time PCR analysis, further validating the accuracy of the assay. Real-time PCR includes DNA extraction and a time-consuming amplification process, whereas our RCCVA assay enables rapid detection without complex preparation. Despite its simplicity and shorter analysis time, it revealed detection patterns comparable with those of real-time PCR. These findings indicate that our system, when combined with an air sampler, can be effectively used for on-site detection of airborne food poisoning bacteria, contributing to improved food hygiene management.

However, all experiments in this study were conducted under controlled laboratory conditions. Real-world environments present far more complex conditions, such as airborne particulates, fluctuating humidity, and heterogeneous microbial communities, that can substantially influence bacterial collection efficiency and amplification performance. In particular, several real-world factors may affect the overall analytical performance, including potential declines in electrostatic sampling efficiency under particulate-rich atmospheric conditions, the presence of enzyme inhibitors or interference from non-target DNA originating from heterogeneous bioaerosol compositions, and variability in thermal lysis efficiency when target bacteria are embedded within complex polluted air or coexist with diverse microbial communities. Therefore, additional field-based validation is necessary to thoroughly assess the robustness, reliability, and practical applicability of the RCCVA system.

2.5. *Performance evaluation under food poisoning contamination conditions*

Building on the laboratory findings, the bacterial detection system was further tested under food poisoning contamination conditions using real food samples to better simulate practical, real-world environments (Fig. 9, Table S5). Airborne bacteria released from food samples incubated with foodborne pathogens, including carrot, pork, beef, chicken, and mixed vegetable, were collected using the air sampler and subjected to downstream analysis. The RCCVA assay generated clear positive signals for all targeted foodborne bacteria. Specifically, the F.I patterns closely matched the Ct values obtained through real-time PCR, confirming that the proposed airborne bacterial detection system provides analytical performance comparable to conventional molecular methods. These findings confirm that the RCCVA assay enables reliable on-site

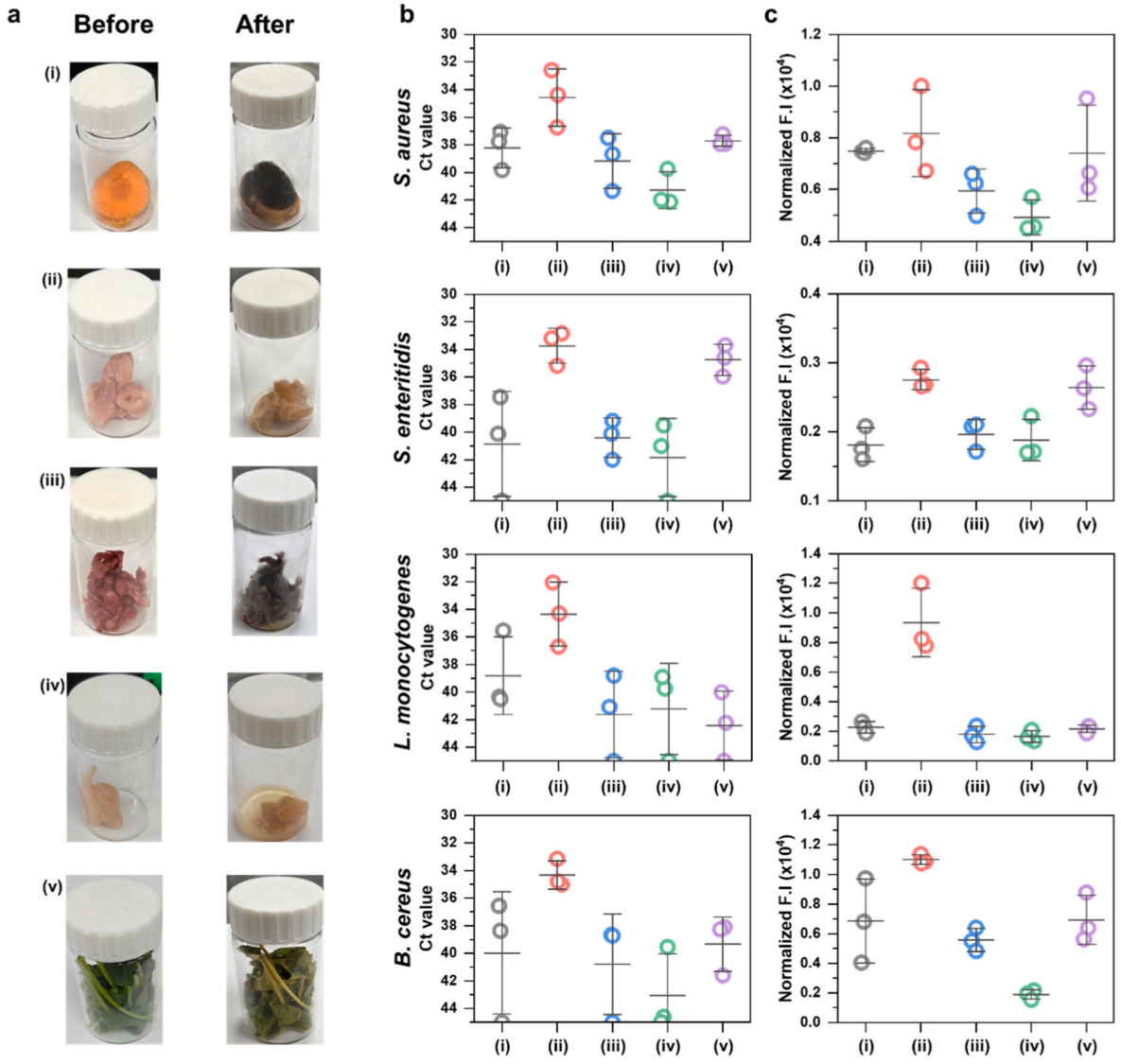

Fig. 9. Detection performance of the RCCVA system under food poisoning contamination conditions. (a) Photographs of food samples before (left) and after (right) incubation: (i) carrot, (ii) pork, (iii) beef, (iv) chicken, and (v) mixed vegetables. **(b)** Normalized F.I at 15 min from CRISPR/Cas12a detection using RPA amplicons. **(c)** RT-PCR results of airborne bacteria collected from food poisoning bacteria-incubated food samples.

detection under complex food poisoning conditions, with performance comparable to standard analytical methods.

2.6. On-site detection of food poisoning bacteria

To verify its on-site applicability, field tests were conducted, where actual food poisoning outbreaks could potentially occur. Three different sites were selected, and the aerosols were collected for 30 min. The collected aerosols were concentrated, thermally lysed, followed by analysis both real-time PCR and RCCVA assay were performed (Fig. 10, Table S6). As a results, *S. aureus* and *L. monocytogenes* were detected all three different locations. *S. aureus* is one of the most commonly detected bacteria in the air, whereas *L. monocytogenes* is known for its resistance to cold environments. Therefore, both *S. aureus* and *L. monocytogenes* were detected during the on-site tests conducted in winter. *B. cereus* is also generally considered as a common airborne bacterium, however, due to the low-temperature and dry condition, only low levels of *B. cereus* were detected at the group catering facility. Overall, the F.I patterns obtained from the RCCVA assay were consistent with the Ct values measured by real-time PCR, confirming that the proposed airborne food poisoning detection system achieves analytical performance comparable to that of conventional detection methods.

3. Conclusion

In this study, we successfully developed a field-deployable monitoring platform for the detection of airborne foodborne bacteria. Airborne bacteria were collected using a self-developed electrostatic air sampler and subsequently analyzed with the RCCVA DNA detection system in combination with a portable isothermal amplification device. This platform eliminates time-consuming procedures and the need for complex PCR instrumentation, while enhancing both sensitivity and specificity. Although the current RCCVA assay involves two sequential steps, that is, amplification and signal read-out, further improvements such as an integration into a unified detection kit or development of true one-pot reactions, may overcome this limitation. Notably, the premixed reagents maintained stable performance for up to 1 month when stored at −20 °C, revealing the feasibility of developing a lyophilized or fully integrated one-pot version of the RCCVA assay in the future. In addition, compared with real-time PCR, the RCCVA assay offers substantially faster detection within 1 h, whereas real-time PCR requires 2~3 h. Moreover, the use of a portable isothermal amplification device

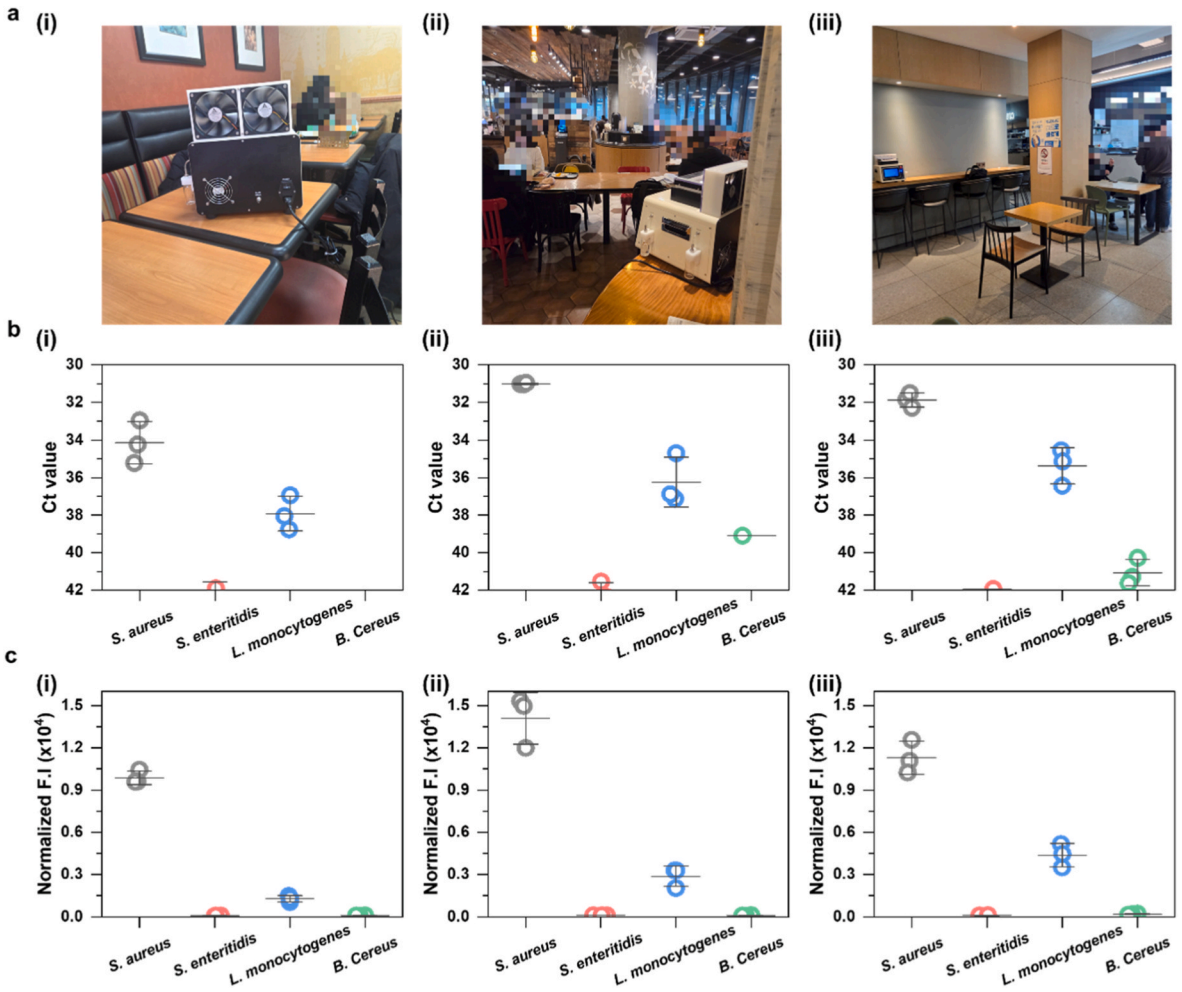

Fig. 10. On-site detection of food poisoning bacteria. (a) Photographs of aerosol captured locations. (i) a franchise restaurant, (ii) a café and (iii) a university cafeteria **(b)** Normalized F.I at 15 min from CRISPR/Cas12a detection using RPA amplicons. **(c)** RT-PCR results of airborne bacteria collected from three different locations.

significantly reduces overall assay cost, further enhancing its suitability for rapid and cost-effective on-site applications. This system, when coupled with a portable detection device, enables early on-site identification of airborne bacteria, including but not limited to foodborne pathogens, thereby helping mitigate public health risks and supporting improvements in both economic and healthcare sectors.

4. Experimental section

4.1. Materials

PBS (tablet) was purchased from Sigma-Aldrich (St. Louis, MO, USA). The QuantiTect SYBR Green PCR Kit was obtained from Qiagen (Hilden, Germany). The TwistAmp® Liquid Basic Kit was purchased from TwistDx (Cambridge, MA, USA). DEPC-treated water was obtained from SolBio (Suwon, Korea), and 10 × TBE buffer was purchased from Biosesang (Hwaseong-si, Gyeonggi-do, Korea). dNTPs (10 mM, each 2.5 mM), DNA oligonucleotides, and the AccuPrep® Genomic DNA Extraction Kit were purchased from Bioneer (Daejeon, Korea). Luria–Bertani high-salt broth (LB broth) was purchased from MBcell (Seoul, Korea). EnGen® Lba Cas12a (Cas12a) and NEBuffer™ r2.1 were purchased from New England BioLabs (Ipswich, MA, USA). Agarose (L.E, analytical grade) was purchased from Promega (Madison, WI, USA) and the O'RangeRuler 100 bp DNA Ladder and 6 × Orange DNA Loading Dye was obtained from Thermo Fisher scientific (Waltham, MA, USA). GelRed® Nucleic Acid Gel Stain (10,000 ×) was purchased from Biotium (Fremont, CA, USA). CRISPR RNAs (crRNA) were purchased from Integrated DNA Technologiew (IDT, Coralville, I.A, USA). Food samples, including carrots, pork, beef, chicken, and mixed vegetables, were purchased from a local grocery store.

4.2. Bacterial culture and genomic DNA (gDNA) extraction

Bacterial stocks of *S. aureus* (ATCC 29213), *S. enteritidis* (ATCC 13076), *L. monocytogenes* (ATCC, 19111), and *B. cereus* (ATCC 21768) were obtained from the American Type Culture Collection (ATCC). *S. aureus, S. enteritidis, L. monocytogenes,* and *B. cereus* were cultured in LB broth at 37 °C with shaking at 150 rpm for 12–18 h. After incubation, the bacterial cultures were harvested and washed three times with phosphate-buffered saline (PBS, 10 mM, pH 7.4) by centrifugation at 13,500 rpm for 5 min. The resulting bacterial pellets were re-suspended in PBS. The concentration of each bacterial suspension (CFU/mL) was estimated by measuring the optical density at 600 nm (OD_{600}) using a UV spectrometer. Serial 10-fold dilutions were prepared in PBS, followed by thermal lysis at 95 °C for 5 min to release nucleic acids. For genomic DNA (gDNA) preparation, bacterial gDNA was extracted using the AccuPrep® Genomic DNA Extraction Kit according to the manufacturer's instructions. The extracted DNA was further diluted through serial 10-fold dilutions using PBS.

4.3. RCCVA assay

Target bacterial gDNA was amplified using the RPA method with the TwistAmp® Liquid Basic Kit (TwistDx), following the manufacturer's protocol. Briefly, the RPA pre-master mix was prepared by combining 25 μL of 2 × Reaction buffer, 5 μL of 10 × Basic E-mix, 9.2 μL of dNTPs and 2.5 μL of 20 × Core reaction mix. Subsequently, 2.4 μL each of the 10 μM forward and reverse primers and 1 μL of target bacterial DNA were added to the pre-master mix. Finally, 2.5 μL of 280 mM magnesium acetate (MgOAc) was added to initiate the reaction. The RPA reaction was conducted at 42 °C for 40 min, followed by incubation at 85 °C for 10 min to terminate the reaction. Amplification was performed using both the CFX Opus 96 real-time PCR system (Bio-Rad) and a portable isothermal amplification device (IsoQuark, RevoSketch), respectively (Fig. S7). When using the IsoQuark device, the post-amplification inactivation step was performed separately at 85 °C. In a separate step, the Cas12a–crRNA complex was prepared by mixing Cas12a (1 μM) and CRISPR RNA (crRNA) in a 1:1 vol ratio, followed by incubation at 37 °C for 1 h to allow complex formation. The CRISPR reaction mixture was then prepared by combining 4 μL of the Cas12a-crRNA complex, 9.2 μL of DEPC-treated water, 0.8 μL of 50 μM FAM-ssDNA-BHQ reporter, and 2 μL of NEBuffer™ r2.1. Following this, 4 μL of RPA product was added to the CRISPR mixture, and FAM fluorescence was measured using both CFX Opus 96 real-time PCR system and IsoQuark, respectively.

The normalized fluorescence intensity (FI) was calculated by the following equation:

$$\text{Normalized FI} = \text{Fluorescence intensity} - \text{Fluorescence intensity at } t = 0 \text{ min (Normalized FI} = \text{FI} - \text{FI}_{t\,=\,0m}) \quad \text{Equation 1}$$

The limit of detection (LOD) was calculated using the following equation:

$$\text{LOD} = 10^{\left(3.3\times\frac{\sigma B}{S}\right)} \quad \text{Equation 2}$$

where, σ ***B*** and *S* are the standard deviation (SD) of the blank solution and slope of calibration curve, respectively.

4.4. Gel electrophoresis

Agarose gel electrophoresis was performed to analyze the RPA products. Agarose gel (2%) was prepared by dissolving 2 g of agarose in 100 mL of 1 × TBE buffer using a microwave oven for 3 min. After cooling the solution to approximately 60 °C, 10 μL of GelRed® Nucleic Acid Gel Stain (10,000 ×) was added prior to casting the gel. The RPA products were mixed with 6 × DNA loading dye, and electrophoresis was performed at 135 V for 50 min.

4.5. Real-time PCR

Real-time PCR analysis was performed as the gold-standard method using the QuantiTect® SYBR® green PCR kit, following the manufacture's protocol. Briefly, each reaction mixture consisted of 2 μL of 10 μM forward primer, 2 μL of 10 μM reverse primer, 4 μL of nuclease-free water, 10 μL of QuantiTect SYBR Green PCR Master Mix, and 2 μL of target bacterial gDNA, for a total volume of 20 μL. Thermal cycling was conducted on a CFX Opus 96 real-time PCR system (Bio-Rad) under the following conditions: initial denaturation at 95 °C for 15 min, followed by 45 cycles of denaturation at 94 °C for 15 s, annealing at 55 °C for 30 s, and extension at 70 °C for 30 s. Fluorescence signals were recorded at each cycle, and quantification cycle (Ct) values were determined. The primer sequences used for this PCR analysis is listed in Table S3.

4.6. Air sampling of food poisoning bacteria

Airborne foodborne bacteria were collected using a Bioaerosol-to-Liquid Sampler (BALS-100, ART Plus, Ltd., Korea) (Fig. S8). The BALS-100 is a high-air-flow-rate (250 L/min) electrostatic sampler used for indoor monitoring of bioaerosols, including bacteria and viruses (An et al., 2024; Choi et al., 2024; Piri et al., 2024;Seo et al., 2025). Fig. 8a illustrates the working principle of the BALS-100. Airborne bacteria entering the sampler were charged by positive ions generated from the discharge electrodes via corona discharge at an applied voltage of 10 kV and subsequently collected on a grounded electrode covered with 25 mL of phosphate-buffered saline (PBS). The operating conditions were selected to protect the captured bacteria from exposure to reactive species generated during the electrostatic collection process and to mitigate dehydration effects associated with dry aerosol collection by employing an aerosol-to-hydrosol sampling approach. To simulate aerosolized bacteria conditions, liquid cultures of the target bacterial strains were mixed and aerosolized. Briefly, *S. aureus, S. enteritidis, L. monocytogenes,* and *B. cereus* were cultured in LB broth at 37 °C with vigorous shaking overnight. Each bacterial culture was washed three times with PBS (10 mM, pH 7.4) by centrifugation at 4000 rpm for 5 min, re-suspended in PBS, and mixed in various compositions. The OD_{600} was measured using a UV spectrometer to determine bacterial concentration, which was then adjusted to 10^7 CFU/mL and transferred into a Collison-type Single-Jet Atomizer (Model 9302; TSI Inc., USA). The BALS-100 was placed in a 50 × 50 × 50 cm chamber, and aerosols were generated using the atomizer with air supplied at a flow rate of 4 L/min. The aerosolized bacteria were then directed into the chamber, which was operated at an airflow rate of 250 L/min for a sampling duration of 30 min. Following collection, the bacterial samples were liquefied and automatically transferred into a vial using an integrated peristaltic pump for downstream analysis (Kim et al., 2021).

4.7. Experimental setup for performance evaluation under food poisoning contamination conditions

The real food samples, including carrots, pork, beef, chicken, and mixed vegetables, were rinsed with 70% ethanol and deionized water for sterilization prior to use. *S. aureus, S. enteritidis, L. monocytogenes,* and *B. cereus* were cultured as described above, and OD_{600} of each culture was measured using a UV spectrometer. Each bacterial strain was diluted to an OD_{600} of 0.1, washed three times with PBS (10 mM, pH 7.4) by centrifugation at 13,500 rpm for 5 min, concentrated again under the same conditions, and then resuspended in 10 μL of PBS. All strains were mixed at an equal ratio (1:1:1:1). The bacterial mixture was then applied to the surface of each food sample, followed by incubation at 37 °C for 5 d. The BALS-100 was placed in a 50 × 50 × 50 cm chamber, and each food poisoning bacteria-incubated food sample was positioned near the sampling device. Airborne bacteria released from each sample were collected for 30 min, liquefied, and automatically transferred into a vial using an integrated peristaltic pump for downstream analysis.

4.8. On-site air sampling of food poisoning bacteria

On-site air sampling was conducted at January 27, 2026, in Seoul, under winter conditions with a minimum temperature of −7.4 °C and a maximum temperature of −0.1 °C, at three different food-service environments to evaluate the field applicability of the proposed RCCVA system. The selected sites included franchise restaurant (temperature: 22.5 °C, humidity: 52%), café (temperature: 25.8 °C, humidity: 30%) and university cafeteria (temperature: 20.5 °C, humidity: 21%). At each location, airborne bacteria were collected for 30 min, liquefied, and automatically transferred into a vial using an integrated peristaltic pump for downstream analysis.

CRediT authorship contribution statement

Yeonwoo Jeong: Conceptualization, Data curation, Writing – original draft. **Jina Lee:** Data curation. **Sangsoo Choi:** Investigation, Methodology. **Dongmin Shin:** Investigation, Methodology. **Soojin Jang:** Methodology, Resources. **Seong Uk Son:** Resources, Validation. **Taejoon Kang:** Funding acquisition. **Juyeon Jung:** Funding acquisition, Resources. **Jungho Hwang:** Funding acquisition, Writing – original draft, Writing – review & editing. **Eun-Kyung Lim:** Conceptualization, Project administration, Writing – original draft, Writing – review & editing.

Declaration of competing interest

The authors declare that they have no known competing financial interests or personal relationships that could have appeared to influence the work reported in this paper.

Acknowledgements

The data from this study are available under the accession number KAP241790 at the Korea BioData Station (K-BDS, http://kbds.re.kr). This research was supported by the National Research Foundation of Korea (NRF) and the National Research Council of Science and Technology (NST), funded by the Korean government (MSIT) (2023R1A2C2005185, RS-2024-00348576, RS-2024-00459749, RS-2025-00554718, 2020R1A5A1018052, and GTL25061-000); by the Korea Evaluation Institute of Industrial Technology (KEIT), funded by the Korean government (MOTIE) (RS-2022-00154853, RS-2024-00432382, and RS-2024-00403563); by the Ministry of Education (RS-2023-00275869); by the Korea Environmental Industry & Technology Institute (KEITI), funded by the Korean government (ME) (2021003370003); by the Korea Health Industry Development Institute (KHIDI), funded by the Korean government (MOHW) (RS-2025-02213315); by the Korea Institute of Planning and Evaluation for Technology in Food, Agriculture and Forestry (IPET), funded by the Korean government (MAFRA) (RS-2024-00401639); and by the KRIBB Research Initiative Program (KGM1322511, KGM1032511). Schematic illustrations were created using BioRender.

Appendix A. Supplementary data

Supplementary data to this article can be found online at https://doi.org/10.1016/j.bios.2026.118571.

Data availability

Data will be made available on request.

References

An, S., Choi, S., Kim, H.R., Hwang, J., 2024. Rapid monitoring of indoor airborne influenza and coronavirus with high air flowrate electrostatic sampling and PCR analysis. Front. Environ. Sci. Eng. 18 (7), 85.

Anaya, C., Church, N., Lewis, J.P., 2007. Detection and identification of bacterial cell surface proteins by fluorescent labeling. Proteomics 7 (2), 215–219.

Arshad, F., Abdillah, A.N., Shivanand, P., Ahmed, M.U., 2024. CeO_2 nanozyme mediated RPA/CRISPR-Cas12a dual-mode biosensor for detection of invA gene in Salmonella. Biosens. Bioelectron. 247, 115940.

Badia-Melis, R., Mc Carthy, U., Ruiz-Garcia, L., Garcia-Hierro, J., Villalba, J.R., 2018. New trends in cold chain monitoring applications-A review. Food Control 86, 170–182.

Bottone, E.J., 2010. Bacillus cereus, a volatile human pathogen. Clin. Microbiol. Rev. 23 (2), 382–398.

Chen, Y., Hu, Y., Lu, X., 2023. Polyethersulfone-based microfluidic device integrated with DNA extraction on paper and recombinase polymerase amplification for the detection of Salmonella enterica. ACS Sens. 8 (6), 2331–2339.

Chen, Z., Ma, L., Bu, S., Zhang, W., Chen, J., Li, Z., Hao, Z., Wan, J., 2021. CRISPR/Cas12a and immuno-RCA based electrochemical biosensor for detecting pathogenic bacteria. J. Electroanal. Chem. 901, 115755.

Choi, S., Piri, A., Jung, J., An, S., Hwang, J., 2024. Determination of airborne influenza virus and coronavirus infectivity using capsid integrity polymerase chain reaction. J. Hazard Mater. 479, 135544.

Daher, R.K., Stewart, G., Boissinot, M., Bergeron, M.G., 2016. Recombinase polymerase amplification for diagnostic applications. Clin. Chem. 62 (7), 947–958.

Dobeic, M., Kenda, E., Mičunovič, J., Zdovc, I., 2011. Airborne listeria spp. in the red meat processing industry. Czech J. Food Sci. 29 (4), 441.

Euromonitor International, 2020. Half the world's new single person households to emerge in Asia Pacific. https://www.euromonitor.com/article/half-the-worlds-new-single-person-households-to-emerge-in-asia-pacific. (Accessed 13 September 2025).

Eurostat, 2025. Household composition statistics. https://ec.europa.eu/eurostat/statistics-explained/index.php?title=Household_composition_statistics. (Accessed 13 September 2025).

Food and Drug Administration, 2020. Accelerated Emergency Use Authorization (EUA) Summary SARS-CoV-2 Assay. Rutgers Clinical Genomics Laboratory, pp. 1–8.

Fu, J., Mo, R., Li, Z., Xu, S., Cheng, X., Lu, B., Shi, S., 2025. An extraction-free one-pot assay for rapid detection of Klebsiella pneumoniae by combining RPA and CRISPR/Cas12a. Biosens. Bioelectron. 267, 116740.

Gast, R.K., Mitchell, B.W., Holt, P.S., 1998. Airborne transmission of Salmonella enteritidis infection between groups of chicks in controlled-environment isolation cabinets. Avian Dis. 315–320.

Gast, R.K., Mitchell, B.W., Holt, P.S., 2004. Detection of airborne Salmonella enteritidis in the environment of experimentally infected laying hens by an electrostatic sampling device. Avian Dis. 48 (1), 148–154.

Glökler, J., Lim, T.S., Ida, J., Frohme, M., 2021. Isothermal amplifications–a comprehensive review on current methods. Crit. Rev. Biochem. Mol. Biol. 56 (6), 543–586.

Ha, T., Enderle, T., Ogletree, D., Chemla, D.S., Selvin, P.R., Weiss, S., 1996. Probing the interaction between two single molecules: fluorescence resonance energy transfer between a single donor and a single acceptor. Proc. Natl. Acad. Sci. 93 (13), 6264–6268.

Huang, T.T., Liu, S.C., Huang, C.H., Lin, C.J., Huang, S.T., 2018. An integrated real-time electrochemical LAMP device for pathogenic bacteria detection in food. Electroanalysis 30 (10), 2397–2404.

James, K., 2023. Reducing food safety risks in meal kits. https://www.food-safety.com/articles/8323-reducing-food-safety-risks-in-meal-kits. (Accessed 13 September 2025).

Jeong, Y., Kim, J., Lee, J., Seo, S.B., Roh, S., Lee, G., Choi, B.G., Bae, N.H., Jung, J., Kang, T., Lee, K.G., Lim, E.K., 2025. Thermo-responsive 3D nanostructures for enhanced performance in food-poisoning bacterial analysis. Mater. Horiz. 12 (2), 451–457.

Ki, J., Kwon, I.H., Lee, J., Lim, J., Jang, S., Son, S.U., Seo, S.B., Oh, S.Y., Kang, T., Jung, J., 2023. A portable smartphone-based colorimetric sensor that utilizes dual amplification for the on-site detection of airborne bacteria. J. Hazard Mater. 460, 132398.

Kim, H.R., An, S., Hwang, J., 2021. High air flow-rate electrostatic sampler for the rapid monitoring of airborne coronavirus and influenza viruses. J. Hazard Mater. 412, 125219.

Kozajda, A., Jeżak, K., Kapsa, A., 2019. Airborne Staphylococcus aureus in different environments—a review. Environ. Sci. Pollut. Control Ser. 26, 34741–34753.

Li, Y., Fan, P., Zhou, S., Zhang, L., 2017. Loop-mediated isothermal amplification (LAMP): a novel rapid detection platform for pathogens. Microb. Pathog. 107, 54–61.

Li, Y., Liu, Y., Tang, X., Qiao, J., Kou, J., Man, S., Zhu, L., Ma, L., 2023. CRISPR/Cas-powered amplification-free detection of nucleic acids: current state of the art, challenges, and futuristic perspectives. ACS Sens. 8 (12), 4420–4441.

Liu, J., Xie, G., Xiong, Q., Mu, D., Xu, H., 2021. A simple and sensitive aptasensor with rolling circle amplification for viable Cronobacter sakazakii detection in powdered infant formula. J. Dairy Sci. 104 (12), 12365–12374.

Liu, L., Zhao, G., Li, X., Xu, Z., Lei, H., Shen, X., 2022. Development of rapid and easy detection of Salmonella in food matrics using RPA-CRISPR/Cas12a method. LWT 162, 113443.

Oliveira, C., Carvalho, L., Garcia, T., 2006. Experimental airborne transmission of Salmonella Agona and Salmonella Typhimurium in weaned pigs. Epidemiol. Infect. 134 (1), 199–209.

Piepenburg, O., Williams, C.H., Stemple, D.L., Armes, N.A., 2006. DNA detection using recombination proteins. PLoS Biol. 4 (7), e204.

Piri, A., Massoudifarid, M., Hwang, J., 2024. Optimal environmental sampling conditions for electrostatic aerosol-to-hydrosol collection of airborne viruses. J. Hazard Mater. 478, 135491.

Pogner, C.-E., Antunes, C., Apangu, G., Bruffaerts, N., Celenk, S., Cristofori, A., Roldán, N.G., Grinn-Gofroń, A., Lara, B., Lika, M., 2024. Airborne DNA: state of the art–established methods and missing pieces in the molecular genetic detection of airborne microorganisms, viruses and plant particles. Sci. Total Environ. 957, 177439.

Qiu, G., Zhang, X., deMello, A.J., Yao, M., Cao, J., Wang, J., 2023. On-site airborne pathogen detection for infection risk mitigation. Chem. Soc. Rev. 52 (24), 8531–8579.

Quijano-Rubio, A., Yeh, H.-W., Park, J., Lee, H., Langan, R.A., Boyken, S.E., Lajoie, M.J., Cao, L., Chow, C.M., Miranda, M.C., 2021. De novo design of modular and tunable protein biosensors. Nature 591 (7850), 482–487.

Seo, S.B., Lee, J., Choi, S., Shin, D., Jang, S., Jeong, Y., Son, S.U., Kang, T., Jung, J., Kim, K., 2025. Onsite detection of airborne antibiotic-resistant bacteria via Cas9 nickase-triggered amplification reactions. J. Hazard Mater., 138850

Seo, S.B., Lee, J., Kim, E., Lim, J., Jang, S., Son, S.U., Jeong, Y., Kang, T., Jung, J., Lee, K. G., 2024. On-site detection of methicillin-resistant Staphylococcus aureus (MRSA) utilizing G-quadruplex based isothermal exponential amplification reaction (GQ-EXPAR). Talanta 275, 126073.

Shetty, P., Ghosh, D., Paul, D., 2017. Thermal lysis and isothermal amplification of Mycobacterium tuberculosis H37Rv in one tube. J. Microbiol. Methods 143, 1–5.

Song, D., Xu, W., Han, X., Wang, H., Zhuo, Y., Liu, J., Zhu, A., Long, F., 2023. CRISPR/Cas12a-powered evanescent wave fluorescence nanobiosensing platform for nucleic acid amplification-free detection of Staphylococcus aureus with multiple signal enhancements. Biosens. Bioelectron. 225, 115109.

Song, S., Wang, X., Xu, K., Xia, G., Yang, X., 2019. Visualized detection of Vibrio parahaemolyticus in food samples using dual-functional aptamers and cut-assisted rolling circle amplification. J. Agric. Food Chem. 67 (4), 1244–1253.

Stein, R., Chirilă, M., 2017. Routes of transmission in the food chain. Foodborne Diseases. Elsevier, pp. 65–103.

Thatcher, S.A., 2015. DNA/RNA preparation for molecular detection. Clin. Chem 61 (1), 89–99.

Unterwurzacher, V., Pogner, C., Berger, H., Strauss, J., Strauss-Goller, S., Gorfer, M., 2018. Validation of a quantitative PCR based detection system for indoor mold exposure assessment in bioaerosols. Environ. Sci. Process. Impacts 20 (10), 1454–1468.

U.S. Census Bureau, 2023. Share of one-person households more than tripled from 1940 to 2020. https://www.census.gov/library/stories/2023/06/more-than-a-quarter-all-households-have-one-person.html. (Accessed 13 September 2025).

Wang, J., Kaur, S., Kayabasi, A., Ranjbaran, M., Rath, I., Benschikovski, I., Raut, B., Ra, K., Rafiq, N., Verma, M.S., 2024. A portable, easy-to-use paper-based biosensor for rapid in-field detection of fecal contamination on fresh produce farms. Biosens. Bioelectron. 259, 116374.

Wang, Y., Ke, Y., Liu, W., Sun, Y., Ding, X., 2020. A one-pot toolbox based on Cas12a/crRNA enables rapid foodborne pathogen detection at attomolar level. ACS Sens. 5 (5), 1427–1435.

Watt, A.E., Browning, G.F., Markham, P.F., Marenda, M.S., 2020. Detection of naturally aerosolized actinobacillus pleuropneumoniae on pig farms by cyclonic air sampling and qPCR. Vet. Microbiol. 250, 108856.

World Health Organization, 2024. Food safety. https://www.who.int/news-room/fact-sheets/detail/food-safety. (Accessed 13 September 2025).

Yan, H., Wen, Y., Tian, Z., Hart, N., Han, S., Hughes, S.J., Zeng, Y., 2023. A one-pot isothermal Cas12-based assay for the sensitive detection of microRNAs. Nat. Biomed. Eng. 7 (12), 1583–1601.

Yang, H., Ledesma-Amaro, R., Gao, H., Ren, Y., Deng, R., 2023. CRISPR-based biosensors for pathogenic biosafety. Biosens. Bioelectron. 228, 115189.

Yang, Q., Zhang, Y., Li, S., Lu, X., Yuan, Y., Zhang, W., 2019. Saltatory rolling circle amplification for sensitive visual detection of Staphylococcus aureus in milk. J. Dairy Sci. 102 (11), 9702–9710.

Yao, J., Zhang, Z., Pei, H., Zhang, T., Ruan, Y., Liu, C., Guo, Y., Gu, S., Xia, Q., 2024. Magnetically modified bacteriophage-triggered ATP release activated EXPAR-CRISPR/Cas14a system for visual detection of Burkholderia pseudomallei. Biosens. Bioelectron. 257, 116334.

Yong, S.-S., Lee, J.-I., Kang, D.-H., 2024. Airborne survival and stress response in Listeria monocytogenes across different growth temperatures. J. Hazard Mater. 468, 133706.

Zhang, L., Bai, H., Zhang, C., He, X., Zou, J., Bai, W., Tang, J., Zhuang, W., Hu, J., Yao, Y., 2025. Dual-mode sensing of Mycobacterium tuberculosis with DNA-functionalized gold nanoparticles and asymmetric RPA-triggered PAM-free CRISPR system. Sensor. Actuator. B Chem. 424, 136920.

Zhao, Y., Chen, F., Li, Q., Wang, L., Fan, C., 2015. Isothermal amplification of nucleic acids. Chem. Rev. 115 (22), 12491–12545.

Zhao, Z., Wang, R., Yang, X., Jia, J., Zhang, Q., Ye, S., Man, S., Ma, L., 2024. Machine learning-assisted, dual-channel CRISPR/Cas12a biosensor-in-microdroplet for amplification-free nucleic acid detection for food authenticity testing. ACS Nano 18 (49), 33505–33519.

Zheng, L., Fan, B., Fu, Y., Wei, J., Ye, Y., Gui, Y., Zhang, S., Wei, Y., Yin, J., Li, J., 2025. Single-tube detection of a foodborne bacterial pathogen using user-friendly portable device. Biosens. Bioelectron. 271, 117035.